

## Article

# Enabling Floating Offshore VAWT Design by Coupling OWENS and OpenFAST

Michael C. Devin <sup>1,\*</sup>, Nicole R. Mendoza <sup>2</sup>, Andrew Platt <sup>2</sup>, Kevin Moore <sup>1</sup>, Jason Jonkman <sup>2</sup>  
and Brandon L. Ennis <sup>1</sup>

<sup>1</sup> Sandia National Laboratories, Albuquerque, NM 87123, USA

<sup>2</sup> National Renewable Energy Laboratory, Golden, CO 80401, USA

\* Correspondence: mcdevin@sandia.gov

**Abstract:** Vertical-axis wind turbines (VAWTs) have a long history, with a wide variety of turbine archetypes that have been designed and tested since the 1970s. While few utility-scale VAWTs currently exist, the placement of the generator near the turbine base could make VAWTs advantageous over traditional horizontal-axis wind turbines for floating offshore wind applications via reduced platform costs and improved scaling potential. However, there are currently few numerical design and analysis tools available for VAWTs. One existing engineering toolset for aero-hydro-servo-elastic simulation of VAWTs is the Offshore Wind ENergy Simulator (OWENS), but its current modeling capability for floating systems is non-standard and not ideal. This article describes how OWENS has been coupled to several OpenFAST modules to update and improve modeling of floating offshore VAWTs and discusses the verification of these new capabilities and features. The results of the coupled OWENS verification test agree well with a parallel OpenFAST simulation, validating the new modeling and simulation capabilities in OWENS for floating VAWT applications. These developments will enable the design and optimization of floating offshore VAWTs in the future.

**Keywords:** vertical-axis wind turbine (VAWT); floating offshore wind turbine (FOWT); OWENS; OpenFAST; hydrodynamics



**Citation:** Devin, M.C.; Mendoza, N.R.; Platt, A.; Moore, K.; Jonkman, J.; Ennis, B.L. Enabling Floating Offshore VAWT Design by Coupling OWENS and OpenFAST. *Energies* **2023**, *16*, 2462. <https://doi.org/10.3390/en16052462>

Academic Editor: Davide Astolfi

Received: 1 February 2023

Revised: 28 February 2023

Accepted: 2 March 2023

Published: 4 March 2023



**Copyright:** © 2023 by the authors. Licensee MDPI, Basel, Switzerland. This article is an open access article distributed under the terms and conditions of the Creative Commons Attribution (CC BY) license (<https://creativecommons.org/licenses/by/4.0/>).

## 1. Introduction

Floating offshore wind turbines are a relatively young and growing technology domain that can play a significant role in decarbonizing the energy sector, particularly in geographic areas where a deep-water wind resource exists. However, additional research and development are needed to reduce the levelized cost of energy (LCOE) of floating offshore wind installations. This goal requires verified and validated design tools to optimize floating offshore wind turbine design and reduce their cost. One commonly used open-source floating offshore wind turbine design and analysis tool is OpenFAST, an aero-hydro-servo-elastic solver developed and maintained by the National Renewable Energy Laboratory (NREL) [1]. OpenFAST is continuously being expanded to support many types of mooring systems, floating platform archetypes, and floating system dynamics and controls. OpenFAST has been extensively verified and validated for three-bladed, horizontal-axis, upwind turbines (HAWTs), but supports limited capability for vertical-axis wind turbines (VAWTs).

Vertical-axis wind turbines have a long history, with a wide variety of turbine archetypes, including the common Darrieus and H-type rotors [2]. While few utility-scale VAWTs currently exist, VAWTs offer some potential advantages over HAWTs, such as being agnostic to the direction of the wind (no yaw error), reduced downstream wake, aerodynamic synergy between turbines in a closely spaced farm, and lower placement of the generator [3]. Recent design studies show that these advantages could provide particular benefit for floating offshore wind turbines, as floating VAWTs have been shown to potentially provide a greater than 20% reduction in LCOE compared to a floating HAWT of equivalent power [4,5].

This development, in addition to increasing interest in leveraging VAWTs for distributed wind applications [2], has spurred renewed interest in VAWT research in the last decade. As Sutherland et al. highlighted the need to optimize commercial-scale designs for VAWTs following the relative absence of the technology since the 1990s [6], researchers have concentrated on developing improved computer software for VAWTs capable of numerically modeling onshore and offshore operation. Researchers have developed and validated several software tools for dynamic floating VAWT simulation, including DeepLines from Principia and IFP Energies Nouvelles [7,8], SIMO-RIFLEX-AC by Cheng et al. [9], FloVAWT by Collu et al. [10], and QBLADE by Marten et al. [11,12]. Owens developed the Offshore Wind Energy Simulator (OWENS) for aero-hydro-servo-elastic VAWT simulation [13], which is currently under further development by Sandia National Laboratories (Sandia).

However, the relatively poor penetration of VAWT technology has kept the validation of these software tools limited, typically using workarounds such as using HAWTs instead of VAWTs or by testing the software in a modularized approach where the aerodynamics, structural dynamics, and hydrodynamics are testing separately of one another. Additionally, validation against VAWT experimental data is scant due to the relative absence of modern experimental testing, especially for floating applications. Howell et al. performed an early comparison of the theoretical tip-speed ratio and rotor performance of a small-scale VAWT in a wind tunnel against CFD and FEA codes, using Fluent and Gambit, respectively [14]. Marten et al. validated the blade performance within QBLADE against historical land-based VAWT data [11]. Recently, Moore and Ennis have validated the aerodynamics and two-way aero-elastic coupling of OWENS against historical Sandia VAWT data, presenting the most comprehensive validation of a VAWT numerical model to date [15,16].

In efforts to continue to improve and validate the OWENS engineering toolset, this work focuses on the development and testing of improved hydrodynamics and mooring dynamics functionality within OWENS. OWENS is currently capable of simulating hydrodynamic and mooring loading for a floating VAWTs via coupling to a modified version of WavEC2Wire [17], but the coupling is not maintained, and the coupling framework used for this in OWENS does not easily allow for coupling to other more common hydrodynamic solvers for offshore wind. To enhance the floating capabilities and user experience of OWENS, an upgrade to the coupling tool is needed. This article describes the coupling of OWENS to the HydroDyn and MoorDyn modules from OpenFAST to improve the coupled aero-hydro-servo-elastic modeling of floating offshore VAWTs and discusses the verification of a coupled OWENS simulation against OpenFAST. The primary goal of this effort is to facilitate the continuing development of OWENS by introducing and validating additional capabilities for floating VAWT applications. By coupling HydroDyn and MoorDyn, OWENS can now model a floating substructure as a rigid body with hydrodynamics and mooring dynamics, thereby enabling studies of the dynamics of the coupled turbine–platform system using validated open-source design tools that are continuously maintained and improved. This article documents the model development (Section 2), as well as the verification procedure and results using the OC4 semi-submersible test case of the upgraded OWENS tool, compared to OpenFAST v3.1.0 (Section 3).

## 2. Numerical Methods

This section describes the existing capabilities and modules of OWENS and OpenFAST relevant to this work, and the methodology used to couple the two programs to enable time domain simulation. To provide context for the following subsections, a module comparison between the software programs is shown in Table 1.

**Table 1.** Modules of OpenFAST and OWENS for modeling different physical phenomena prior to the coupling accomplished in this work.

Physical Phenomena	OpenFAST	OWENS
Structural dynamics	ElastoDyn	GyricFEA
Wind inflow	InflowWind	VAWTAero
Aerodynamics	AeroDyn	VAWTAero or CACTUS
Hydrodynamics	HydroDyn	WavEC2Wire
Mooring dynamics	MoorDyn	WavEC2Wire

## 2.1. OWENS

OWENS is an engineering toolset for VAWT aero-hydro-servo-elastic numerical simulation written in the Julia programming language. OWENS uses a modular framework that interfaces structural dynamics, aerodynamics, servo-dynamics, hydrodynamics, and mooring dynamics modules to predict the full system response of a land-based or floating VAWT, with a block-Gauss–Seidel iterative method to stabilize results across modules. It can model and analyze a wide variety of VAWT configurations and composite structures in both the modal and unsteady domains with full two-way coupling between all subsystems. Additionally, the software is written so much of the code can propagate automatic gradients, thus enabling significant enhancements for numerical optimization approaches.

### 2.1.1. Structural Solver

GyricFEA is the structural dynamics module encompassing the original functionality of OWENS. Using a user-defined finite element mesh and structural properties, GyricFEA predicts the elastic deformation of a VAWT of any arbitrary configuration subject to external and inertial forces. The module uses a robust finite element method, applying Timoshenko beam theory to each element of a VAWT using a Newmark- $\beta$  method to solve for the element dynamics in the reference frame of the VAWT rotor. GyricFEA can also account for rigid body displacements of a VAWT on a floating platform by applying spin softening and Coriolis forces to the structure.

### 2.1.2. Aerodynamics

The aerodynamics portion of OWENS, VAWTAero, includes a set of reformulated actuator cylinder and double multiple streamtube models that overcome previous issues regarding accuracy for 3D curved blades, and an improved numerical method for unsteady analysis [15]. These methods are coupled and validated for two-way coupled aero-elastic analysis [16]. One-way coupling to the vortex method tool CACTUS has also been maintained as an option.

The coupling of OWENS with AeroDyn, the aerodynamics module in OpenFAST, is also under development through a separate project. This coupling will enable OWENS to make use of the aerodynamic modeling capability recently implemented in OpenFAST for VAWTs, including two-way coupling to a free-wake vortex method coupled to multiple unsteady airfoil aerodynamics models.

### 2.1.3. Servo Dynamics

OWENS includes a basic interface to calculate the generator and drivetrain torque based on the user-defined drivetrain stiffness, damping, and control torque law. The program is also able to interface with custom profiles provided by users for dictating the generator and drivetrain response. Features including additional control systems are under development.

### 2.1.4. Hydrodynamics and Moorings

OWENS is coupled to a modified version of the WavEC2Wire software developed by Marco Alves, with the drivetrain PTO loads replaced by the tower base reaction loads [17]. WavEC2Wire receives the tower base reaction loads as inputs from GyricFEA, calculates

the effects of the hydrodynamics and mooring of a user-defined platform, and returns the platform motions to GyricFEA. However, this current approach presents various shortcomings. First, the coupling requires users to set up and run a simulation of the modified version of WavEC2Wire simultaneously with an OWENS simulation on another computer, which presents significant overhead and accessibility issues for many users. Second, many standard hydrodynamic modeling tools for floating wind systems (including OpenFAST) use rigid body motions of the platform as inputs, while this coupling requires OWENS to instead use tower base reaction loads as inputs, limiting the capability of OWENS to be coupled to many other existing hydrodynamics design tools. Additionally, the version of WavEC2Wire applied in previous work is limited to a linear wave model and a quasi-static mooring function, impacting the accuracy of simulations of extreme and fatigue loading conditions.

## 2.2. OpenFAST

OpenFAST is a physics-based engineering tool for simulating the coupled dynamic response of wind turbines in various wind and wave environments [1]. OpenFAST provides the framework that couples physics-based engineering modules for aerodynamics, multimember, multibody hydrodynamics, control and electrical system (servo) dynamics, and structural dynamics to enable coupled nonlinear aero-hydro-servo-elastic simulation in the time domain. OpenFAST enables the analysis of a range of wind turbine configurations, including two- or three-blade horizontal-axis rotor, pitch or stall regulation, rigid or teetering hub, upwind or downwind rotor, and lattice or tubular tower. The wind turbine can be modeled on land or offshore on fixed-bottom or floating substructures. OpenFAST also supports linearization of the solution. The OpenFAST modules that have been coupled to OWENS through this work are as follows:

### 2.2.1. InflowWind

InflowWind is a module for processing different types of wind-inflow that are supported by OpenFAST. InflowWind supports arbitrary wind directions and several wind file formats, including uniform, binary TurbSim full field, binary Bladed-style full field, and HAWC formatted binary full-field turbulent wind files. Additionally, InflowWind supports an internally calculated steady wind model. Uniform wind files support simulations involving deterministic transient gusts. Turbulent full-field wind files support spatially and temporally varying wind inflow.

At each time step, InflowWind receives from either the stand-alone driver code or OpenFAST the coordinate position of various points, and then InflowWind returns the undisturbed wind-inflow velocities at these positions. There are no states in the module: each wind velocity component is calculated as a function of the input coordinate positions and internal time-varying parameters, undisturbed from interacting with the wind turbine. For full-field turbulent wind data types, InflowWind uses Taylor's frozen turbulence hypothesis—valid only for stationary conditions—to translate wind defined in two-dimensional planes into three spatial dimensions, using the mean wind speed as the advection speed.

### 2.2.2. HydroDyn

HydroDyn is a hydrodynamics module applicable to both fixed-bottom and floating offshore substructures [18]. HydroDyn allows for multiple approaches to calculating the hydrodynamic loads on a structure: a potential-flow theory solution, a strip-theory solution, or a hybrid combination of the two. Waves generated internally within HydroDyn can be regular (periodic) or irregular (stochastic), and long-crested (unidirectional) or short-crested (with wave energy spread across a range of directions). Wave elevations or full wave kinematics can also be generated externally and used within HydroDyn. Internally, HydroDyn generates waves analytically for finite depths using first-order (linear Airy) or first- plus second-order wave theory [19] with the option to include directional

spreading, albeit with wave kinematics only computed in the domain between the flat seabed and still water level. Wave stretching will also be introduced in an upcoming version. The second-order hydrodynamic implementations include time-domain calculations of difference-frequency terms (mean- and slow-drift) and sum-frequency terms. To minimize computational expense, fast Fourier transforms (FFTs) are applied in the summation of all wave frequency components.

The potential-flow solution is applicable to multiple bodies and/or substructures or members of substructures that are large relative to a typical wavelength and amplitude, assuming an inviscid, irrotational, incompressible fluid in constant water depth. The potential-flow solution involves either frequency-to-time-domain transforms or fluid-impulse theory. In the former, potential-flow hydrodynamic loads include linear hydrostatic restoring, the added mass and damping contributions from linear wave radiation (including free-surface memory effects), and the incident-wave excitation from first- and second-order diffraction (Froude-Krylov and scattering). The hydrodynamic coefficients (first and second order) required for the potential-flow solution are frequency-dependent and must be supplied by a separate frequency-domain panel code (e.g., WAMIT) from a precomputation step. The radiation memory effect can be calculated either through direct time-domain convolution or through a linear state-space approach, with a state-space model derived through the SS\_Fitting preprocessor. A state-space option was recently added for wave excitation as well. The second-order terms can be derived from the full difference- and sum-frequency quadratic transfer functions (QTFs) or the difference-frequency terms can be estimated via Standing et al.'s extension to Newman's approximation, based only on first-order coefficients [20]. The use of fluid-impulse theory is not yet documented.

The strip-theory solution may be preferable for substructures or members of substructures that are small in diameter relative to a typical wavelength. Strip-theory hydrodynamic loads can be applied across multiple interconnected members, each with possible incline and taper, and are derived directly from the undisturbed wave and current kinematics at the displaced position of the substructure. The strip-theory loads include the relative form of Morison's equation for the distributed fluid-inertia, added-mass, and viscous-drag components. Additional distributed load components include axial loads from tapered members and static buoyancy loads about the displaced position. Hydrodynamic loads can also be applied as lumped loads on member endpoints (joints). It is also possible to include flooding or ballasting of members, and the effects of marine growth. The hydrodynamic coefficients required for this solution come through user-specified dynamic-pressure, added-mass, and viscous-drag coefficients.

The analysis of many substructures and sea conditions applicable to floating offshore wind can be made more accurate by augmenting the hydrodynamic loads from a potential-flow theory with the loads brought on due to viscous effects from a strip-theory solution. For this, the viscous-drag component of the strip-theory solution may be included with the potential-flow theory solution in HydroDyn. Another option available is to supply a global damping matrix (linear or quadratic) to the system to represent this effect.

When HydroDyn is coupled to OpenFAST or OWENS, HydroDyn receives the position, orientation, velocities, and accelerations of the (rigid or flexible) substructure at each coupling time step and then computes the hydrodynamic loads (including added mass) and returns them back to OpenFAST or OWENS.

### 2.2.3. MoorDyn

MoorDyn is an open-source lumped-mass mooring line model that can be driven independently or by OpenFAST. MoorDyn supports arbitrary line interconnections, clump weights and floats, and different line properties. The model accounts for internal axial stiffness and damping forces, weight and buoyancy forces, hydrodynamic forces from Morison's equation, and vertical spring-damper forces from contact with the seabed. The formulation supports inclusion of wave kinematics in the hydrodynamic force calculations

when coupled to HydroDyn in OpenFAST, but this feature is not presently included in the coupling to OWENS.

MoorDyn uses a lumped-mass approach to discretize the cable dynamics over the length of the mooring line. A cable is broken up into  $N$  uniformly sized line segments connecting  $N + 1$  node points. Each segment of the cable has identical properties of unstretched length, diameter, density, and Young's modulus. Different cables can have different sets of properties, and cables can be connected at the ends, enabling mooring systems with interconnected lines.

Hydrodynamic loads are calculated directly at the node points rather than at the segment centers. This ensures damping of transverse cable vibrations having a wavelength of twice the cable segment length. To approximate the cable direction at the node points, the cable tangent at each node is assumed to be the average of the tangent directions of the two adjacent cable elements.

### 2.3. Numerical Interface Architecture

The core algorithms of the OpenFAST modules are written in Fortran, while OWENS is written in pure Julia. Julia can call C code directly, so we developed a C-based module interface to enable the OpenFAST modules to communicate with OWENS. The calling interface libraries described herein are specific to the Julia, and new libraries will need to be generated for other languages to communicate properly with the Fortran module library.

As the OpenFAST modules have been previously verified and validated independent of this work, we desired to modify the existing Fortran modules as little as possible. Instead, we developed new wrappers that pass data appropriately between OpenFAST modules and C-based drivers. Figure 1 illustrates the relationship between the Fortran module subroutines of OpenFAST and OWENS, using HydroDyn as an example. A new Fortran-C module interface library (HydroDyn\_C), written in Fortran, is needed to convert Fortran data types into C-based data types, store data used internally in HydroDyn, and transition from pass by reference (Fortran) to pass by value (C). An interface library file in Julia, HydroDyn\_Lib, is needed to interface the C code to a version readable by OWENS using the `ccall` syntax in Julia.

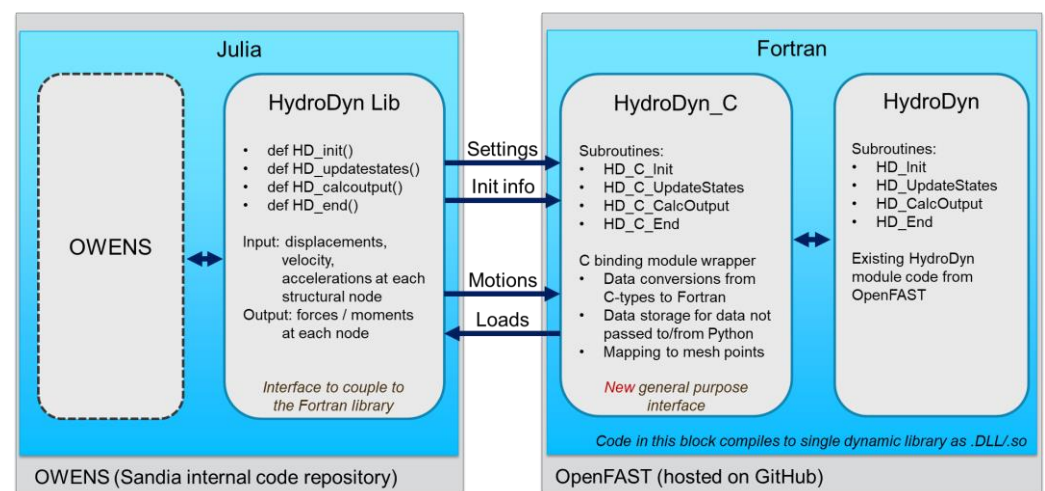


**Figure 1.** High-level schematic representation of coupling the existing versions of OWENS and HydroDyn. Motions and loads are exchanged at each time step of the simulation.

In summary, we made the following high-level changes needed to couple each OpenFAST module to OWENS:

- Wrote one new C-bindings interface library written in Fortran, interfacing OpenFAST to C,
- Wrote one new C-Julia interface library, interfacing C to OWENS, and

- Compiled a dynamic library to call the compiled C-bindings interface within the C-Julia interface library

We also wrote an external driver in Python to use as an example for each module for potential future bindings between OpenFAST modules and other C-based languages. In total, nine new files were written and added to both the OpenFAST and OWENS code repositories to support interfacing the OpenFAST HydroDyn, MoorDyn, and InflowWind modules with OWENS (the InflowWind coupling is not included in the OWENS verification test in Section 3). A more detailed diagram is shown in Figure 2, which also shows Python and Julia interface libraries.

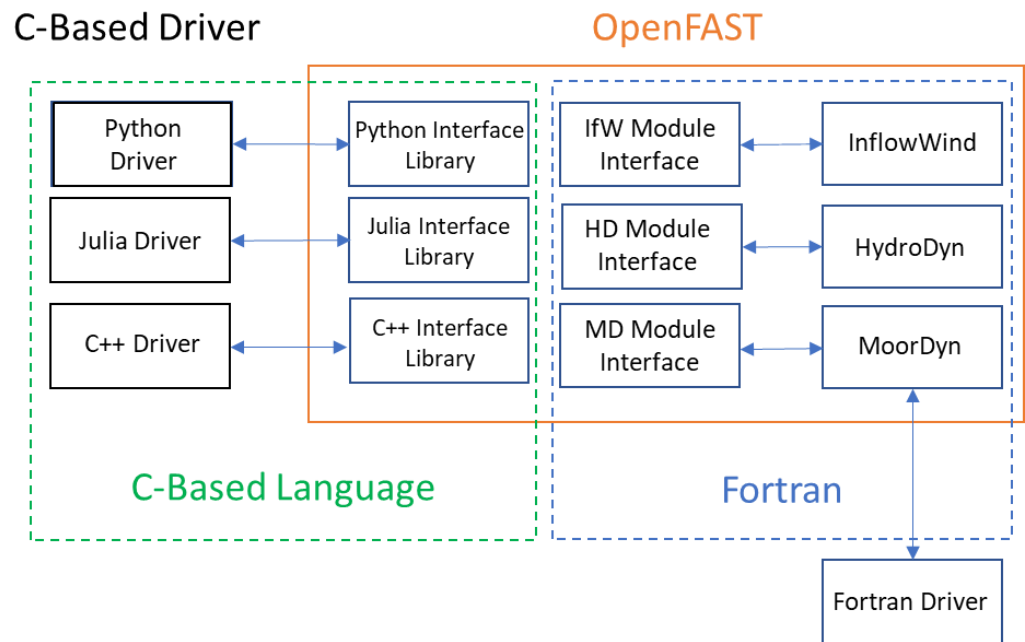


**Figure 2.** Diagram of module library relationships and languages (IfW = InflowWind; HD = HydroDyn; MD = MoorDyn).

### 2.3.1. OpenFAST Module Interface Library

The interface libraries and their associated calling libraries support the conversion of variable types, formats, and addressing when passing them through the function calls. The module interface libraries are written in Fortran and heavily use the Fortran ISO\_C\_BINDING module alongside the module source files. Each of the four main subroutines—Init(), UpdateStates(), CalcOutput(), and End()—are C-bound, using

```
SUBROUTINE module_C_INIT(variable list) BIND (C, NAME =
    'module_C_INIT')
```

The input and output variables are standardized according to the OpenFAST framework and include time indexing and state information. The overall flow of the script for each of the four main subroutines is as follows:

- Convert the input variable types and formats;
- Perform any preparation steps (initialization, allocation, etc.);
- Call the associated main module subroutine;
- Convert the output variable types and formats, set output variable values;
- Clean up (deletion, deallocation, etc.).

Both MoorDyn and HydroDyn include the conversion of the multidimensional platform mesh in OpenFAST to a single point for OWENS, and vice versa. Performing this conversion correctly involved employing subroutines from the NWTC library and the module source files. These modules assume small angular displacements less than about

+/- 17 degrees or less for platform motions (this limitation could be overcome with the use of full direction cosine matrices for the orientations but would require significant changes to the internal code).

The source code for OpenFAST module C-bindings interface libraries are available in the OpenFAST repository within the respective module source directory (i.e., `modules/hydrodyn/src/HydroDyn_C_Bindings.f90` for HydroDyn). These may be compiled using the CMake build system or Visual Studio projects provided in the repository.

### 2.3.2. OWENS Module Interface Library

The interface libraries transitioning the C code to Julia is tightly coupled to its associated module interface library. The libraries make extensive use of the built-in C interface to Julia with the following structure:

- Pass in variable values defined in the driver program;
- For `moduleName_updateStates()`, `moduleName_calccutput()`, and `moduleName_end()`, verify the module has been initialized (i.e., confirm the `moduleName_init()` function has been called);
- Convert input and output variable types between C and Julia using built-in Julia C types (`Cfloat`, `Cstring`, etc.);
- Use the `ccall` function to access the C code with the converted inputs and in-place outputs;
- Check for any errors that may have occurred at the Fortran level and handle them within Julia.

The libraries specific for calling each of the OpenFAST modules in OWENS are available in the `OpenFASTWrappers.jl` repository on GitHub [21]. The example Python interfacing libraries for are available in the OpenFAST repository within the respective module source directory (i.e., `modules/hydrodyn/python-lib/hydrodyn_library.py`) [22].

### 2.3.3. Example External Driver

The driver code to call the OpenFAST module subroutines within OWENS is described below in Section 2.4, but is currently only accessible via a private Sandia repository. Instead, an example of the external driver file is included in the OpenFAST repository to demonstrate how to successfully call the module-specific subroutines within Python in a very similar manner. The driver file primarily utilizes the interface library file while minimizing additional dependencies. It supports `.dll`, `.dylib`, and `.so` files. Its overall structure is:

- Import the module-specific interface library file;
- Initialize and/or instantiate the class and variables;
- Call `moduleName_C_Init()`;
- Step through time, calculating the outputs at each time step using `moduleName_C_calcOutputs()` and `moduleName_C_updateStates()`;
- When finished, close out and clean up with `moduleName_C_End()`.

Examples of Python drivers calling the OpenFAST module libraries through the interfaces mentioned above are available as module level regression tests in the OpenFAST repository (i.e., `reg_tests/r-test/modules/hydrodyn/hd_py_5MW_OC4Semi_WSt_WavesWN/hydrodyn_driver.py`) [22].

## 2.4. Numerical Coupling Algorithm

As OWENS and OpenFAST both utilize a loose coupling modularized framework, the integration of the OpenFAST modules into OWENS is theoretically relatively straightforward. However, as mentioned in Section 2.1.4, the OWENS hydro-elastic coupling framework has previously assumed tower base loads to be the inputs for the coupled hydrodynamic module, while HydroDyn and MoorDyn expect rigid body motions of the floating platform as inputs. As a result, we substantially modified the hydro-elastic



coupling methodology in the OWENS source code to enable coupling to HydroDyn and MoorDyn.

Section 2.4.1 discusses the modifications made to the hydro-elastic module interface within OWENS, allowing GyricFEA to interface with the HydroDyn and MoorDyn C-based libraries discussed above. Section 2.4.2 discusses the interface changes to the meshing within GyricFEA required to his interface change requires OWENS to natively represent a floating platform. Finally, Section 2.4.3 documents the changes made to the time domain simulation framework in the OWENS glue code to integrate the new hydro-elastic coupling methodology and meshing approach with its existing VAWT simulation capabilities.

#### 2.4.1. Coupling Interface

Enabling OWENS to directly interface with the HydroDyn and MoorDyn interface libraries required several notable changes to its existing hydro-elastic coupling routine. First, we shifted the modular partitioning point from the tower base to the fluid-structure boundary at the platform. This is due to HydroDyn and MoorDyn expecting inputs and outputs at the platform reference point (a term derived from WAMIT), which is intractable if partitioning at the tower base. Second, we inverted the hydro-elastic I/O interface in OWENS, which required completely rebuilding the coupling framework within the glue code. This was accomplished by representing the platform as a separate mesh within the OWENS structural module GyricFEA, as GyricFEA natively receives external loads as inputs and returns motions as outputs. This meshing strategy is discussed in greater detail in the next section.

Finally, we replaced the method used to achieve numerical convergence and stability. This was needed because the previously used block-Gauss–Seidel method is ill-suited to handle the added mass term interfacing across the modules. Namely, the added mass contributions to the hydrodynamic loading on the platform are dependent on the accelerations of the platform (calculated in GyricFEA), but the accelerations of the platform are themselves dependent on the hydrodynamic loading (calculated in HydroDyn). The block-Gauss–Seidel method has no easy way to handle this tight coupling of the added mass in a way that will converge unconditionally when it is split across two modules [23]. To resolve this, a new solve procedure has been implemented for the GyricFEA–HydroDyn coupling within OWENS using a block-Newton–Raphson solver to account for the residuals each program produces for its outputs as its inputs are perturbed. This is a very similar procedure used to couple HydroDyn to ElastoDyn within OpenFAST.

The Newton–Raphson solver procedure operates as follows:

1. GyricFEA calculates structural motions (including the platform accelerations  $\ddot{\mathbf{q}}_{old}$  and  $\ddot{\boldsymbol{\theta}}_{old}$ ) using the platform reference point loads  $\mathbf{F}_{old}$  extrapolated from the previous time step in six degrees of freedom. No platform loads are used on the first time step of the simulation.
2. MoorDyn calculates mooring loads  $\mathbf{F}_{mooring}$  in six degrees of freedom for the current time step using the structural motions computed in step 1.
3. The total platform loads from the previous time step (or zero, if it is the first time step of the simulation) and the platform motions from step 1 are saved to the input vector  $\hat{\mathbf{u}}$ , where

$$\hat{\mathbf{u}}[1 : 6] = \frac{\mathbf{F}_{old}}{1,000,000} \quad (1)$$

$$\hat{\mathbf{u}}[7 : 12] = [\ddot{\mathbf{q}}_{old}, \ddot{\boldsymbol{\theta}}_{new}] \quad (2)$$

The platform loads saved in  $\hat{\mathbf{u}}$  are divided by a factor of 1,000,000 to be in the same order of magnitude as the accelerations.

4. HydroDyn calculates the hydrodynamic loads  $\mathbf{F}_{hydro_{new}}$  for the current time step, and GyricFEA calculates the structural motions (including the platform accelerations  $\ddot{\mathbf{q}}_{new}$

and  $\ddot{\theta}_{new}$ ) for the current time step. The new hydrodynamic loads are recombined with the mooring loads to get the new total platform loads:

$$F_{new} = F_{hydro_{new}} + F_{mooring} \quad (3)$$

5. The solver calculates the residual  $\hat{u}_{resid}$  between the outputs calculated in step 4 and  $\hat{u}$ :

$$\hat{u}_{resid}[1 : 6] = \frac{F_{old} - F_{new}}{1000000} \quad (4)$$

$$\hat{u}_{resid}[7 : 12] = [\ddot{q}_{old} - \ddot{q}_{new}, \ddot{\theta}_{old} - \ddot{\theta}_{new}] \quad (5)$$

6. The solver calculates the Jacobian of  $\hat{u}$ ,  $J_{\hat{u}}$ . Each column of  $J_{\hat{u}}$  is calculated by perturbing the primary causal load or acceleration input, running the relevant program to solve for the output, solving for the residual between the old outputs and the perturbed outputs, and taking the difference between  $\hat{u}_{resid}$  and the new perturbed residual;
7. The change in loads/accelerations,  $\delta\hat{u}$ , is solved with

$$\delta\hat{u} = J_{\hat{u}}^{-1}(-\hat{u}_{resid}) \quad (6)$$

8. The solver updates  $\hat{u}$  to  $\hat{u}'$ , with

$$\hat{u}' = \hat{u} + \delta\hat{u} \quad (7)$$

9. GyricFEA and HydroDyn run again using the updated loads/accelerations contained in  $\hat{u}'$  to get the final outputs at the current time, which are returned to the top-level glue code in OWENS as the time marching proceeds.

#### 2.4.2. Updated OWENS Mesh

As OpenFAST and OWENS have substantially different structural solve procedures, coupling HydroDyn and MoorDyn to OWENS requires careful mesh representation and translation of different inputs and outputs. Fundamentally, the meshing approach in OWENS for a floating VAWT uses two finite element meshes:

- A simple, three-node mesh representing the platform, with zero distributed mass, quasi-infinite stiffness, and two concentrated masses.
- A complex mesh composed of many nodes, representing everything at the turbine base and above (i.e., the “topside”).
- The locations of the three nodes represent the platform center of gravity, the platform reference point, and the turbine base (which must be the top node). The two concentrated masses on the platform mesh are the  $6 \times 6$  mass matrices of the platform and topside, each representing the respective mass and inertia of each subsystem. The platform and topside concentrated masses are applied at the platform center of gravity and turbine base nodes, respectively. The hydrodynamic and mooring loads are applied at the platform reference node.

The coupling between the two meshes is shown in Figure 3. The topside mesh has boundary conditions at the bottom node (the turbine base) fixing it into place, but the rigid body motions of the platform are received from the platform mesh at each time step and are used to:

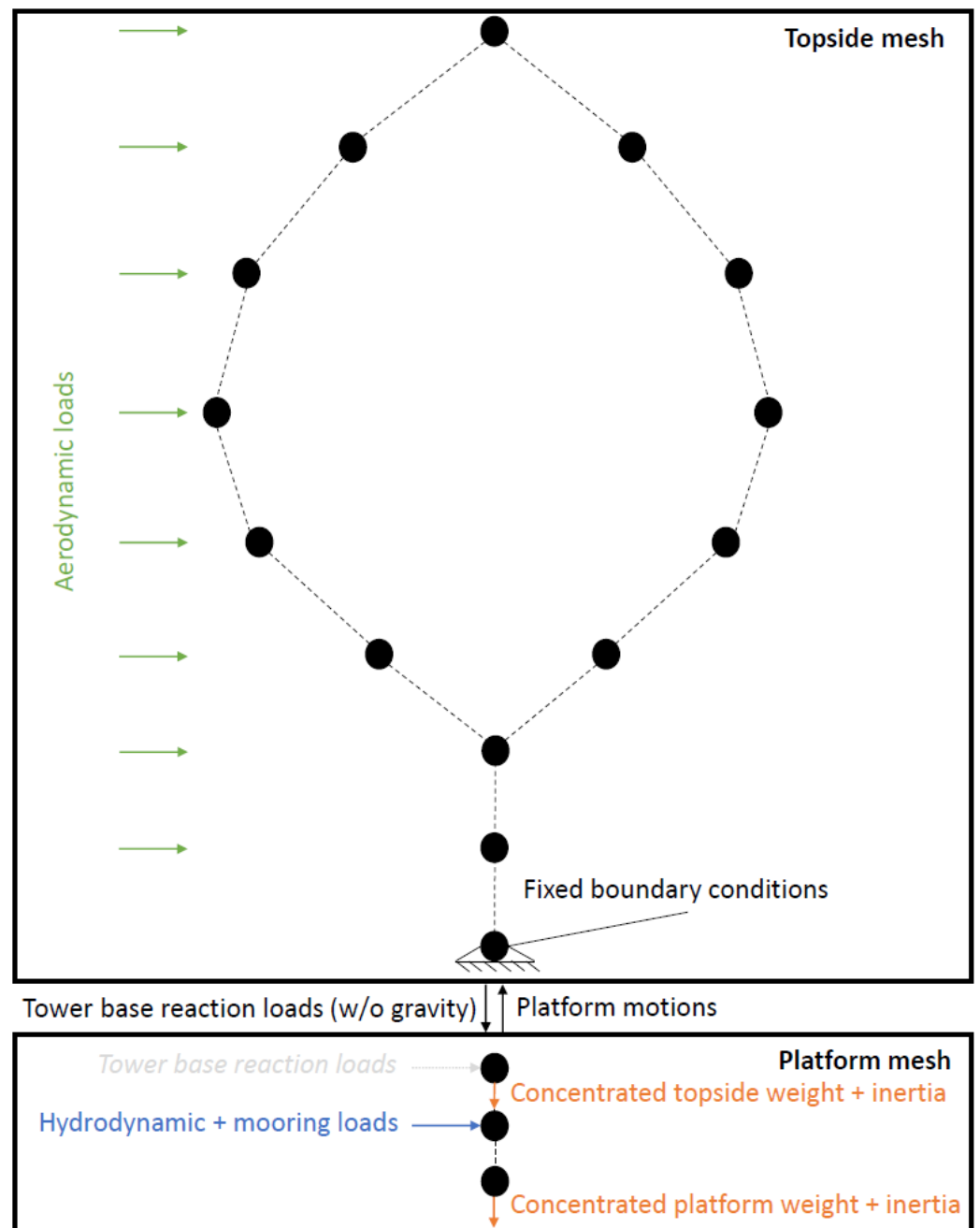


**Figure 3.** A visual representation of the two meshes used in a coupled turbine–platform OWENS simulation.

1. Create the rotation matrix from the global to the hub reference frame (along with the hub rotation information at the current time step), which is used in the OWENS solver for the topside structure.
2. Generate the Coriolis and spin softening forces needed on the topside mesh to account for the deflection of the platform in the rotating hub reference frame, in addition to the force due to the acceleration of the platform.

This approach of separating the two meshes is taken for several reasons. First, representing a rigid body platform in the same finite element mesh as a more flexible topside results in a difference in stiffness of several orders of magnitude between different elements of the mesh, which can result in simulation instability. Second, the block-Newton–Raphson method used for the GyricFEA–HydroDyn coupling described in Section 2.4.1 requires

several calls to GyricFEA, which scales linearly with the number of elements. If the entire structure were represented in a single mesh, the many elements of the topside being evaluated in the block-Newton–Raphson approach would be computationally inefficient with no obvious gain. Finally, GyricFEA natively operates in the rotor reference frame, while the coupled OpenFAST modules operate in the global reference frame. Separating the two meshes allows the platform mesh to operate in the global reference frame and the topside mesh to operate in the rotor reference frame; the platform motions and tower base reaction loads only need to rotate at the transfer between the meshes, making the bookkeeping in the source code more straightforward.

#### 2.4.3. Coupled OWENS Solution

The process flow between the two meshes is shown in Figure 4. The topside mesh solves for structural motions using displacements from the previous time step and aerodynamic loads from the current time steps via a Newmark- $\beta$  approach [24], iterated using the Gauss–Seidel method until the difference between the nodal displacements and rotor rotation to the previous iteration are sufficiently small and can be considered converged. This is identical to the solution method GyricFEA has used previously in OWENS. Upon convergence, the opposite of the reaction loads at the tower base due to the aerodynamic loading (i.e., ignoring the effects of gravity) are transferred to the tower base node on the platform mesh as an external load, and the platform motions are solved using the block-Newton–Raphson method laid out above. The platform motions are then sent to the topside mesh, repeating the Gauss–Seidel/Newmark- $\beta$  solve with the new platform motions now accounted for. The new converged results are saved and used to predict values for the next time step.

It is important to note that the topside mesh is evaluated in the hub reference frame while the platform mesh is evaluated in the global reference frame. Thus, the tower base reaction force is rotated into the global frame from the hub frame when transferring to the platform mesh, and vice versa for the platform motions when transferring to the topside mesh. The rotation matrix is extrapolated from the platform displacements and the rotor rotation is calculated in the previous time step.

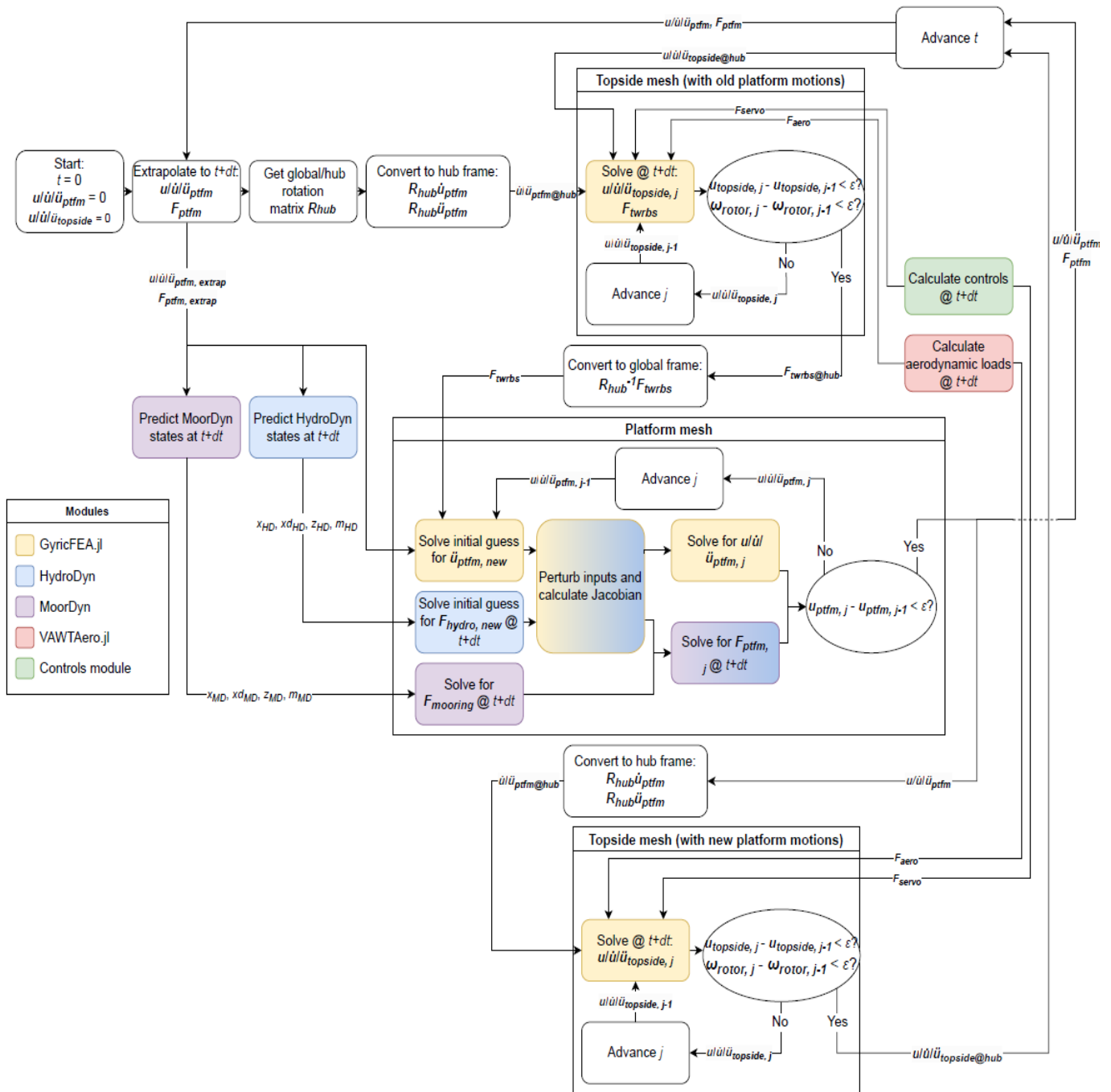


Figure 4. Workflow of a single time step of a coupled OWENS simulation.

### 3. Load Case Results and Discussion

A code-to-code verification was necessary to ensure the proper and correct response of the new coupled code. In this verification, OpenFAST results were considered the baseline truth, and the newly coupled OWENS results were compared to them for accuracy. Since OpenFAST cannot easily simulate a floating offshore VAWT, we developed a test case based on the OC4 DeepCwind verification case. The modeled system consists of a flexible central tower and semisubmersible platform excited by an identical prescribed time-varying tower-top forcing function and wave seed to ensure equivalent load conditions between the two programs.

### 3.1. Model Definition

#### 3.1.1. Turbine

A modified NREL 5-MW Reference Wind Turbine is used for the verification test case. The entire rotor/nacelle assembly (RNA). A full description of the unmodified reference turbine is available in [25]. See Section 3.1.4 for further details on the modifications made for the verification test.

#### 3.1.2. Platform

The OC4 DeepCwind semisubmersible floating offshore platform was used for the verification test case. This platform was developed during OC4 Phase II and is based on the DeepCwind floating wind system. It is illustrated in Figure 5. A complete description of the semisubmersible platform is available in [26]. The platform is assumed to be a rigid body in both programs.



**Figure 5.** DeepCwind floating wind system design.

#### 3.1.3. Mooring

The mooring system used in the verification test case is identical to that used in OC4 Phase II [26]. This system uses three 835 m-long mooring lines symmetrically placed 120° apart. Each mooring line is attached to a fairlead located at the top of the base columns at a depth of 14 m below the still water level and at a radius of 40.87 m from the platform centerline. The water depth is 200 m.

#### 3.1.4. Model Simplifications

This verification case includes the following simplifications to the OC4 system to easily represent equivalent floating systems in both OpenFAST and OWENS:

- The aerodynamics module and InflowWind module in both tools are turned off.
- In lieu of wind loading, a prescribed loading profile is applied at the yaw bearing in global coordinates (i.e., not following the tower-top orientation).
- All RNA degrees of freedom are turned off; only the tower and platform degrees of freedom are enabled.
- The entire RNA is represented as a single-point, 350,000 kg lumped mass at the yaw bearing with no center of mass offset or rotational inertia.

- The tower mode shapes in ElastoDyn have been updated to reflect the lumped mass assumption above.

### 3.2. Verification Load Cases

#### 3.2.1. Verification Objectives and Framework

The goal of this verification test is to ensure that OWENS, when coupled to HydroDyn and MoorDyn, produces results close to a corresponding simulation in OpenFAST v3.1.0 with only minor differences. The results are considered acceptable if (a) total time response root mean square errors are less than 20% per parameter, (b) ultimate loads for the upwind mooring line and tower base shear force (particularly critical values for floating offshore wind turbine design analysis) are less than 10%, and (c) the frequency responses are aligned with spectral peaks occurring at very similar frequencies. These criteria test whether the new OWENS hydro-elastic coupling methodology is valid while accounting for expected minor errors due to fundamental differences in the structural solvers in OpenFAST versus OWENS. For this test, a 10-min simulation is performed in both OWENS and OpenFAST using the floating system model described in Section 3.1 with zero initial tower and platform displacement. Both programs use HydroDyn as of the v3.1.0 release of OpenFAST alongside MoorDyn v2.a8. The resulting rigid body displacements of the platform, mooring tensions, tower base loading, tower top loading, and wave elevation are compared between OWENS and OpenFAST to validate the coupling methodology.

#### 3.2.2. Orientation and Coordinate Systems

Both programs use identical global coordinate systems:  $x$  is positive in the nominal zero-degree downwind wind and wave direction and is parallel to the still water level;  $z$  is vertical and positive upwards (opposite gravity); and  $y$  is computed via the right-hand rule (directed left when looking downwind).

#### 3.2.3. Wind Environment

While no wind excitation is directly input in the simulation, the prescribed time-series forcing function described in Section 3.1.4 is generated using a turbulent wind profile (using IEC turbulence Class B and a wind shear power law exponent of 0.2) with an average wind speed of 12 m/s on the equivalent rigid land-based system and variable speed and collective blade-pitch control enabled. The forcing functions consist of prescribed time series of three forces and three moments representing the resulting aerodynamic loading applied to the RNA at the yaw bearing in global coordinates.

#### 3.2.4. Wave Environment

The wave environment used for the verification test case is an irregular white noise excitation with the white noise parameters displayed in Table 2. These wave conditions are identical to those used in load cases 2.6 and 3.7 of IEA Wind Task 30 OC4 Phase II [27].

**Table 2.** Wave environment white noise parameters.

Parameter	Units	Value
Wave height	m	1.2646
Wave direction spreading	-	none
Wave time step	s	0.2
Wave spectrum lower frequency limit	rad/s	0.314159
Wave spectrum upper frequency limit	rad/s	1.570796
Power spectral density	m <sup>2</sup> /Hz	1.0
HydroDyn WaveSeed (1)	-	123,456,789
HydroDyn WaveSeed (2)	-	RANLUX

### 3.3. Verification Results and Discussion

The time domain and frequency domain comparisons of OWENS coupled to OpenFAST for the verification test are shown in Figures 6 and 7, respectively. These results reflect the coupling algorithm outlined in Section 2.4 and the load case definition in Section 3.2, and thus do not include the interface to the InflowWind module. Wave elevation results are excluded here, as OWENS and OpenFAST produce identical wave histories in HydroDyn in both cases. In general, the simulation results between the two tools show good time response matching and excellent frequency response matching for the outputs considered, with some notable discrepancies highlighted in the following subsections:

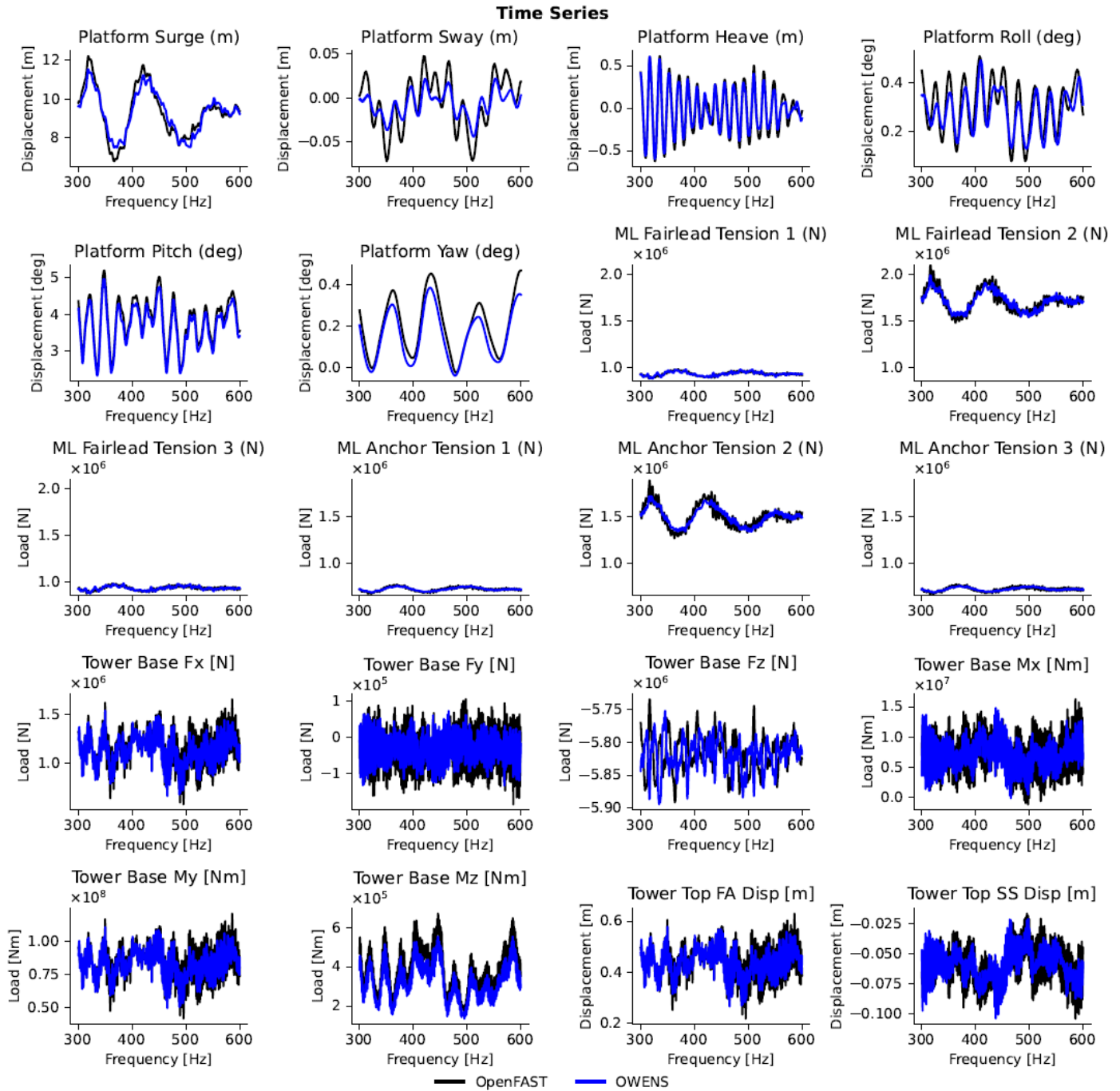


Figure 6. Time-series results of the OWENS-OpenFAST verification test.



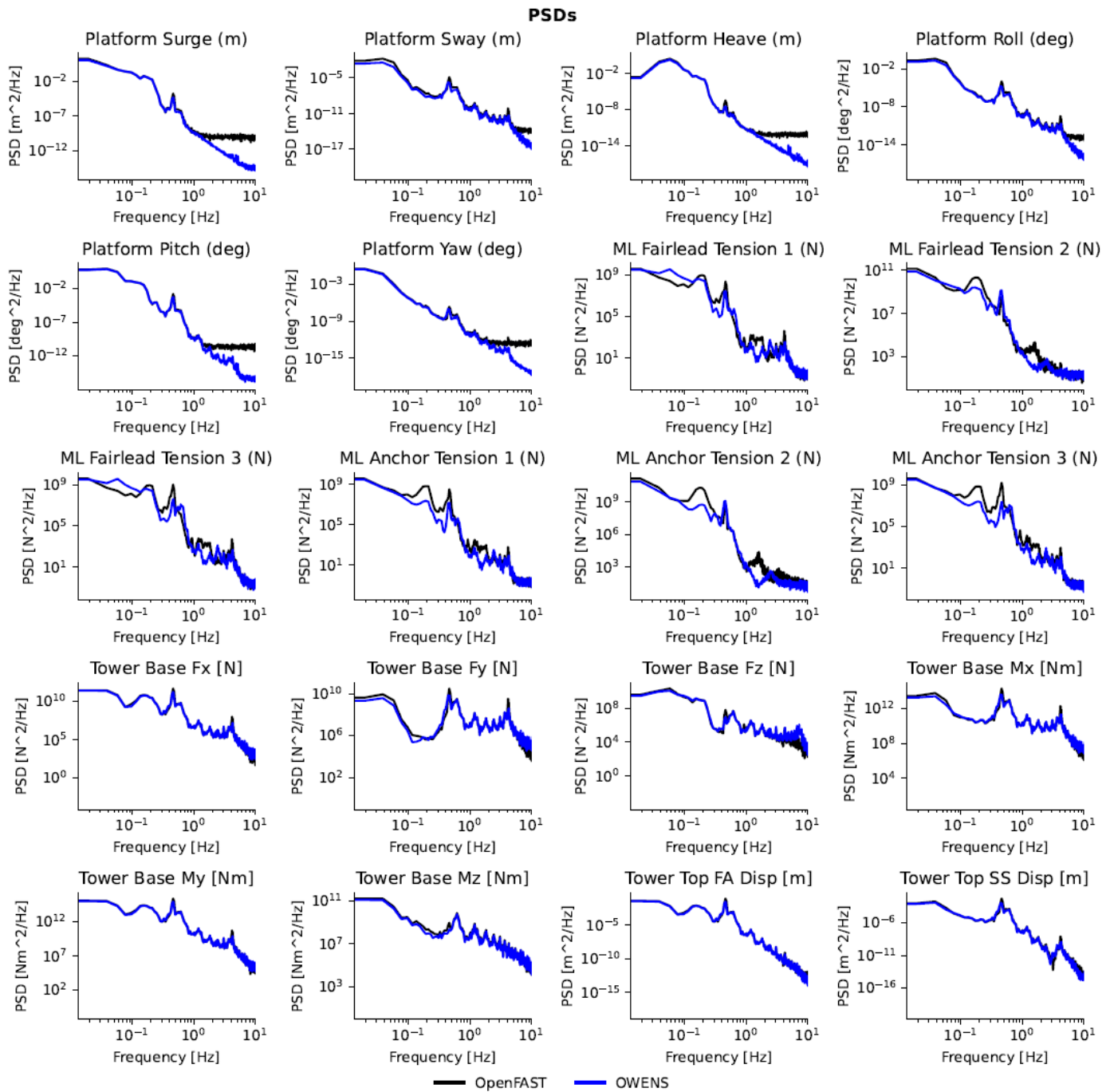
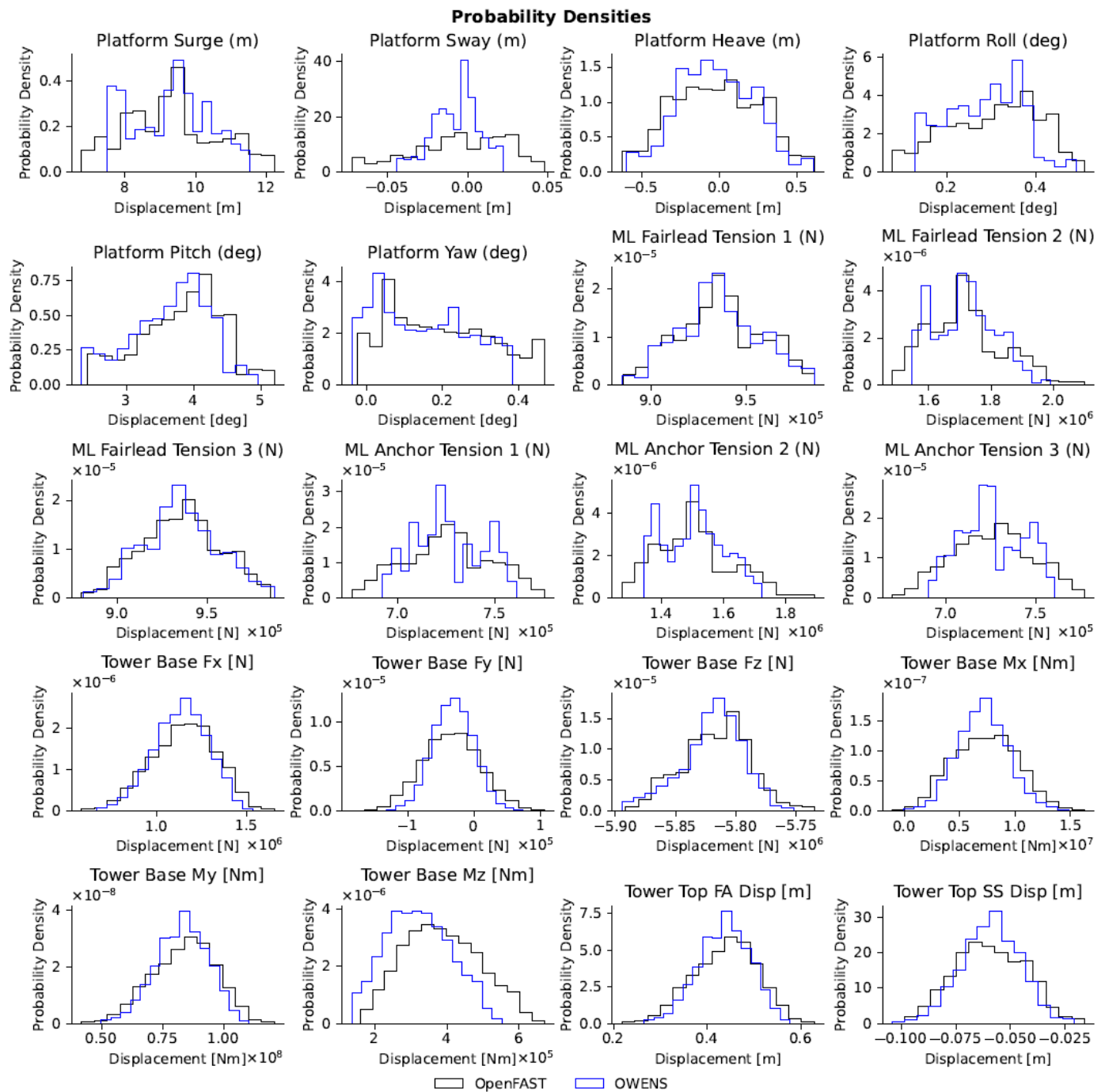


Figure 7. Power spectral densities (PSD) of the OWENS-OpenFAST verification results.

### 3.3.1. Platform Motions

OWENS underpredicts the platform motion response, visually most notable in the platform sway and yaw responses (though this increased visual discrepancy are largely due to the magnitudes in these degrees of freedom being very small). This is also illustrated by the narrower range bands in the OWENS results in the probability density functions, shown in Figure 8.



**Figure 8.** Probability densities of the OWENS-OpenFAST verification results.

These underpredictions are perhaps due to the differences in how structural deflections are calculated in OWENS compared to OpenFAST (the platform motions are ultimately calculated in the structural module in both programs). The Newmark- $\beta$  solver in GyricFEA within OWENS solves for displacement using loads and effective stiffness, from which velocity and acceleration are derived for each time step. Alternatively, ElastoDyn in OpenFAST solves for acceleration using generalized active and inertial forces via Kane’s dynamics, which is integrated to find velocity and displacement. As such, OWENS may not be accounting for changes in acceleration due to higher-order effects that OpenFAST is able to capture, resulting in smaller overall magnitudes despite the frequency response mapping well. This may be propagating either from GyricFEA directly, the resulting changes in wave loading due to the transfer of these motions to state variables in HydroDyn and

MoorDyn, or both; it is challenging to determine with certainty due to the complex coupled hydro-elastic effects.

This could also explain why the high-frequency response of the platform motions is noticeably more energetic in OpenFAST compared to OWENS, though there is relatively little energy in this frequency range.

### 3.3.2. Mooring Tensions

The time response of the mooring tensions between the programs aligns well with the mean value and low-frequency response of the platform, but OWENS inaccurately predicts the spectral response in the wave frequency range. This is visible in both Figure 6 by the less noisy waveforms in the mooring tensions, as well as explicitly in Figure 7 from 0.05 to 0.25 Hz. This is likely due to the MoorDyn library in OWENS missing wave kinematics to excite the mooring lines in this frequency band, with hydrodynamic load calculations for the mooring lines instead assuming still water. Inclusion of the wave kinematics is present in the HydroDyn-MoorDyn coupling within the OpenFAST glue code, which is impossible to implement in the individual HydroDyn and MoorDyn module libraries used in OWENS due to their standalone nature. However, these responses are important to the accuracy of the coupling, and methods to account for the wave kinematics within the OWENS glue code are being discussed and will be implemented in a future OWENS release.

Additionally, OWENS underpredicts high frequency responses of all mooring lines, most notably around 1.5 Hz. This may be due to unaccounted higher-order effects on the platform motions, which impact the state variables in MoorDyn due to differences in the structural module solve procedures, as discussed in Section 3.3.1. However, this frequency range is much less energetic than the low- and wave-frequency ranges.

### 3.3.3. Tower Motions and Loads

Similar to the platform motion time response, tower motions and base loads in OWENS are generally smaller amplitude than in OpenFAST. This is likely due to the differences in the Newmark- $\beta$  structural solver in OWENS and the Kane's dynamics solver in OpenFAST, as discussed in Section 3.3.1. The time response of the "Tower Base Fz" parameter noticeably deviates as well. This is likely due to a bug discovered in OWENS, where a small phase shift occurring in the beginning of the OWENS simulation caused by the topside nodes shifting down a small amount. Since the coupling between the platform and topside meshes in OWENS do not account for gravity on the initial topside solve each time step, this transient load is isolated to the outputs and does not affect the behavior of the platform mesh. This transient load will be addressed in future OWENS release.

### 3.3.4. Statistical Error

The root mean square error normalized to the range of each parameter is plotted in Figure 9, showing that all parameters fall under 20% except for the "Tower Base Fz" parameter. Ultimate load errors are included in Table 3 for the upwind mooring line and tower base shear forces, showing these loads in OWENS are predicted within 10% of the loads given in OpenFAST. Finally, the spectral peaks align to the same frequencies in OpenFAST and OWENS except the wave-frequency range of the mooring line tensions. These two deviations from the test criteria have known causes discussed in Sections 3.3.2 and 3.3.3, and will be corrected in an upcoming OWENS release, at which point these results will be considered acceptable by the criteria defined in Section 3.2.1.

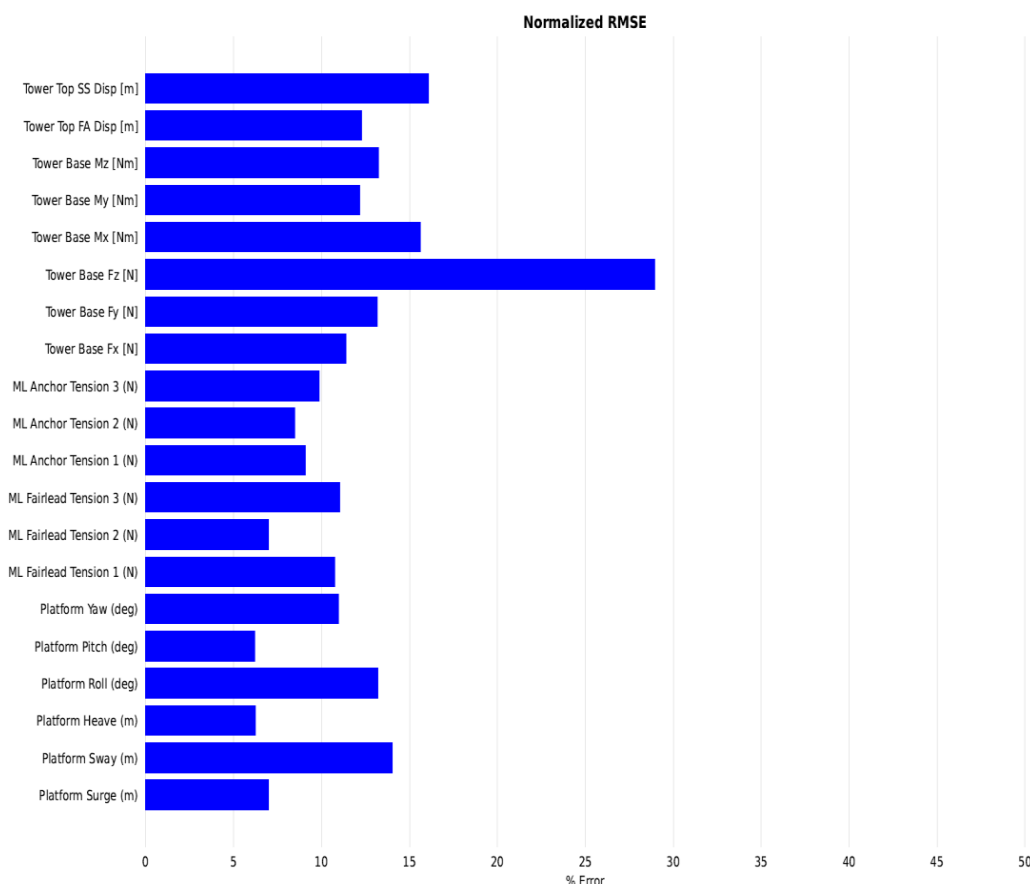


Figure 9. Normalized root mean square error of the OWENS results relative to the OpenFAST results.

Table 3. Ultimate load percentage error of OWENS results relative to the OpenFAST results.

Parameter	% Error
ML Fairlead Tension 2	5.32
ML Anchor Tension 2	9.02
Tower Base Fx	7.16

Overall, we consider the OWENS results to be in good agreement with OpenFAST. These data confirm that the coupling methodology between OWENS and the HydroDyn and MoorDyn modules operates as desired, with differences resulting from known causes to be corrected in a future release or are relatively minor, enabling the modules to be confidently incorporated into the OWENS toolset for future floating VAWT analysis and design.

#### 4. Conclusions and Future Work

This work demonstrates a new hydro-elastic coupling methodology in OWENS to model floating offshore vertical-axis wind turbine systems with coupling to OpenFAST modules in the time domain. This builds upon other recent work validating the OWENS aerodynamic and aero-elastic coupling [16,17], and will allow OWENS to be applied to floating VAWT analysis in a better supported and more accessible manner. Results show good agreement between the coupled OWENS code and an equivalent OpenFAST simulation, with discrepancies in the tower base vertical loading and wave frequency mooring line response identified and to be corrected in an upcoming OWENS release to fully validate the code coupling. OWENS validation efforts will continue as capabilities of the code continue to expand and floating VAWT experimental data become available,

enabling researchers and industry partners to model floating offshore VAWT designs more easily and accurately to reduce the levelized cost of energy and improve deployment.

The OpenFAST code changes described herein are publicly accessible through the OpenFAST GitHub repository and will be maintained as part of the OpenFAST code base. The new files may also be modified appropriately for utilizing other C-based languages with the OpenFAST Fortran modules. The Julia wrappers coupling the OpenFAST C binaries to OWENS are also publicly accessible via the OpenFASTWrappers.jl GitHub repository and will be maintained as OWENS continues development.

Immediate future work will focus on improving the accuracy of the coupled OWENS code by correcting the vertical tower node behavior and adding wave kinematics coupling for the mooring lines, as described in Section 3.3. Further work will then primarily focus on continued OWENS validation. Extended validation for the floating functionality in severe environmental conditions is needed and will be subject to future code-to-code comparisons. Additionally, validation efforts for both land-based and floating capabilities in OWENS are being planned for newer VAWT experimental data as they become available.

**Author Contributions:** Conceptualization, N.R.M., J.J., M.C.D., K.M. and B.L.E.; methodology, all authors.; software, N.R.M., M.C.D., A.P. and K.M.; formal analysis, N.R.M., J.J. and M.C.D.; investigation, all authors; resources, all authors; writing (original draft preparation), N.R.M. and M.C.D.; writing (review and editing), all authors; visualization, N.R.M., A.P. and M.C.D.; supervision, J.J. and B.L.E.; project administration, J.J. and B.L.E.; funding acquisition, J.J. and B.L.E. All authors have read and agreed to the published version of the manuscript.

**Funding:** This work has been funded by the U.S. Department of Energy Advanced Research Projects Agency for Energy (ARPA-E) under the Aerodynamic Turbines, Lighter and Afloat, with Nautical Technologies and Integrated Servo-control (ATLANTIS) Program. This work was authored in part by the National Renewable Energy Laboratory, operated by Alliance for Sustainable Energy, LLC, for the U.S. Department of Energy (DOE) under Contract No. DE-AC36-08GO28308. Sandia National Laboratories is a multimission laboratory managed and operated by National Technology & Engineering Solutions of Sandia LLC, a wholly owned subsidiary of Honeywell International Inc. for the U.S. Department of Energy's National Nuclear Security Administration under contract DE-NA0003525.

**Data Availability Statement:** All data generated in this research were generated using OpenFAST v3.1.0 with MoorDyn v2a8 and OWENS, developed by the National Renewable Energy Laboratory and Sandia National Laboratories, respectively. OpenFAST is freely available on GitHub at <https://github.com/OpenFAST/openfast> (accessed on 20 January 2023). OWENS can be acquired via a commercial license from Sandia National Laboratories. See <https://ip.sandia.gov/technology.do/techID=314> (accessed on 20 January 2023) for more information.

**Conflicts of Interest:** The authors declare no conflict of interest. The funders had no role in the design of the study; in the collection, analyses, or interpretation of data; in the writing of the manuscript; or in the decision to publish the results.

**Disclaimer:** This paper describes objective technical results and analysis. Any subjective views or opinions that might be expressed in the paper do not necessarily represent the views of the U.S. Department of Energy or the United States Government. The U.S. Government retains and the publisher, by accepting the article for publication, acknowledges that the U.S. Government retains a nonexclusive, paid-up, irrevocable, worldwide license to publish or reproduce the published form of this work, or allow others to do so, for U.S. Government purposes.

## References

1. Jonkman, B.; Mudafort, R.M.; Platt, A.; Branlard, E.; Sprague, M.; Jonkman, J.; Hayman, G.; Vijayakumar, G.; Buhl, M.; Ross, H.; et al. OpenFAST/openfast: OpenFAST v3.1.0, Zenodo [code]. 2022. Available online: <https://zenodo.org/record/6324288#.ZAFU2h9BxPY> (accessed on 20 January 2023).
2. Kumar, R.; Raahemifar, K.; Fung, A.S. A critical review of vertical axis wind turbines for urban applications. *Renew. Sustain. Energy Rev.* **2018**, *89*, 281–291. [[CrossRef](#)]
3. Hand, B.; Kelly, G.; Cashman, A. Aerodynamic design and performance parameters of a lift-type vertical axis wind turbine: A comprehensive review. *Renew. Sustain. Energy Rev.* **2021**, *139*, 110699. [[CrossRef](#)]

4. Paquette, J.; Barone, M. *Innovative Offshore Vertical-Axis Wind Turbine Rotor Project*; SAND2012-2777C; Sandia National Laboratories, Copenhagen: Albuquerque, NM, USA, 2012.
5. Griffith, D.T.; Barone, M.; Paquette, J.; Owens, B.; Bull, D.; Simao-Ferreira, C.; Goupee, A.; Fowler, M. *Design Studies for Deep-Water Floating Offshore Vertical Axis Wind Turbines*; SAND2018-7002; Sandia National Laboratories: Albuquerque, NM, USA, 2018.
6. Sutherland, H.J.; Berg, D.E.; Ashwill, T.D. *A Retrospective of VAWT Technology*; SAND2012-0304; Sandia National Laboratories: Albuquerque, NM, USA, 2012.
7. Le Cunff, C.; Heurtier, J.-M.; Piriou, L.; Berhault, C.; Perdrizet, T.; Teixeira, D.; Ferrer, G.; Gilloteaux, J.-C. Fully Coupled Floating Wind Turbine Simulator Based on Nonlinear Finite Element Method-Part I: Methodology. In Proceedings of the ASME 2013 32nd International Conference on Ocean, Offshore and Arctic Engineering, Nantes, France, 9–14 June 2013.
8. Perdrizet, T.; Gilloteaux, J.-C.; Teixeira, D.; Ferrer, G.; Piriou, L.; Cadiou, D.; Heurtier, J.-M.; Le Cunff, C. Fully Coupled Floating Wind Turbine Simulator Based on Nonlinear Finite Element Method-Part II: Validation Results. In Proceedings of the ASME 2013 32nd International Conference on Ocean, Offshore and Arctic Engineering, Nantes, France, 9–14 June 2013.
9. Cheng, Z.; Madsen, H.A.; Gao, Z.; Moan, T. A Fully Coupled Method for Numerical Modeling and Dynamic Analysis of Floating Vertical Axis Wind Turbines. *Renew. Energy* **2017**, *107*, 604–619. [[CrossRef](#)]
10. Collu, M.; Borg, M.; Shires, A.; Rizzo, F.N.; Lupi, E. FloVAWT: Further Progresses on the Development of a Coupled Model of Dynamics for Floating Offshore VAWTs. In Proceedings of the ASME 2014 33rd International Conference on Ocean, Offshore and Arctic Engineering, ASME, San Francisco, CA, USA, 8–13 June 2014.
11. Marten, D.; Wendler, J.; Pechlivanoglou, G.; Nayeri, C.N.; Pascherit, C.O. QBLADE: An Open Source Tool for Design and Simulation of Horizontal and Vertical Axis Wind Turbines. *Int. J. Emerg. Technol. Adv. Eng.* **2013**, *3*, 264–269.
12. Marten, D.; Saverin, J.; Behrens de Luna, R.; Perez-Becker, S. “Validation Cases and Examples,” QBlade Documentation. 2021. Available online: [https://docs.qblade.org/src/validation/index\\_val.html](https://docs.qblade.org/src/validation/index_val.html) (accessed on 20 January 2023).
13. Owens, B.C. Theoretical Developments and Practical Aspects of Dynamic Systems in Wind Energy Applications. Ph.D. Thesis, Texas A&M University, College Station, TX, USA, 2013.
14. Howell, R.; Qin, N.; Edwards, J.; Durrani, N. Wind Tunnel and Numerical Study of a Small Vertical Axis Wind Turbine. *Renew. Energy* **2009**, *35*, 412–422. [[CrossRef](#)]
15. Moore, K.R.; Ennis, B.L. Vertical-Axis Wind Turbine Steady and Unsteady Aerodynamics for Curved Deforming Blades. *AIAA J.* **2022**, *60*, 189–196.
16. Moore, K.R.; Ennis, B.L. Aeroelastic Validation of the Offshore Wind Energy Simulator for Vertical-Axis Wind Turbines. *Wind. Energy Sci. Discuss.* **2022**, 1–28. [[CrossRef](#)]
17. Fowler, M.J.; Owens, B.; Bull, D.; Goupee, A.J.; Hurtado, J.; Griffith, D.T.; Alves, M. Hydrodynamic Module Coupling in the Offshore Wind Energy Simulation (OWENS) Toolkit. In Proceedings of the ASME 2014 33rd International Conference on Ocean, Offshore and Arctic Engineering, ASME, San Francisco, CA, USA, 8–13 June 2014.
18. Jonkman, J.; Robertson, A.N.; Hayman, G.J. HydroDyn User’s Guide and Theory Manual. NREL Technical Report. Available online: <https://openfast.readthedocs.io/en/main/source/user/hydrodyn/index.html> (accessed on 1 March 2022).
19. Sharma, N.; Dean, R. Second-order directional seas and associated wave forces. *Soc. Pet. Eng. J.* **1981**, *4*, 129–140. [[CrossRef](#)]
20. Standing, R.G.; Brending, W.J.; Wilson, D. Recent Developments in the Analysis of Wave Drift Forces, Low-Frequency Damping and Response. In Proceedings of the 79th Annual OTC, Houston, TX, USA, 27–30 April 1987.
21. GitHub.com. 2022. SNL-WaterPower/OpenFASTWrappers.jl: A Repository Containing Julia Wrappers for Standalone In-flowWind, HydroDyn, and MoorDyn Modules from OpenFAST. Available online: <https://github.com/SNL-WaterPower/OpenFASTWrappers.jl/tree/main> (accessed on 20 January 2023).
22. GitHub.com. 2022. OpenFAST/openfast: Main Repository for the NREL-Supported OpenFAST Whole-Turbine and FAST.Farm Wind Farm Simulation Codes. Available online: <https://github.com/OpenFAST/openfast/tree/main> (accessed on 10 August 2022).
23. Matthies, H.G.; Niekamp, R.; Steindorf, J. Algorithms for Strong Coupling Procedures. *Comput. Methods Appl. Mech. Eng.* **2006**, *195*, 2028–2049. [[CrossRef](#)]
24. Zhou, Z.; Wen, Y.; Chenzhi, C.; Zeng, Q. *Step-by-Step Integration Method. Fundamentals of Structural Dynamics*; Elsevier: Amsterdam, The Netherlands, 2021; pp. 245–266.
25. Jonkman, J.; Butterfield, S.; Musial, W.; Scott, G. *Definition of a 5-MW Reference Wind Turbine for Offshore System Development*; National Renewable Energy Lab.(NREL): Golden, CO, USA, 2009. [[CrossRef](#)]
26. Robertson, A.; Jonkman, J.; Masciola, M.; Song, H.; Goupee, A.; Coulling, A.; Luan, C. *Definition of the Semisubmersible Floating System for Phase II of OC4*; National Renewable Energy Lab.(NREL): Golden, CO, USA, 2014. [[CrossRef](#)]
27. Robertson, A.; Jonkman, J.; Vorpahl, F.; Popko, W.; Qvist, J.; Frøyd, L.; Chen, X.; Azcona, J.; Uzunoglu, E.; Guedes Soares, C.; et al. Offshore Code Comparison Collaboration Continuation Within IEA Wind Task 30: Phase II Results Regarding a Floating Semisubmersible Wind System. In Proceedings of the International Conference on Offshore Mechanics and Arctic Engineering, San Francisco, CA, USA, 8–13 June 2014; Volume 9B, p. V09BT09A012.

**Disclaimer/Publisher’s Note:** The statements, opinions and data contained in all publications are solely those of the individual author(s) and contributor(s) and not of MDPI and/or the editor(s). MDPI and/or the editor(s) disclaim responsibility for any injury to people or property resulting from any ideas, methods, instructions or products referred to in the content.